Scientia Iranica F (2016) 23(6), 3135–3144

SCIENTIA IRANICA

Sharif University of Technology
Scientia Iranica
Transactions F: Nanotechnology
www.scientiairanica.com

Fabrication and study of UV-shielding and photocatalytic performance of uniform TiO_2/SiO_2 core-shell nanofibers via single-nozzle co-electrospinning and interface sol-gel reaction

O. Nakhaei[a,b], N. Shahtahmassebi[a,b,*], M. Rezaee Roknabadi[a] and M. Behdani[a]

a. *Department of Physics, School of Science, Ferdowsi University of Mashhad, Mashhad, P.O. Box 9177948974, Iran.*
b. *Nano Research Center, Ferdowsi University of Mashhad, Mashhad, P.O. Box 9177948974, Iran.*

Received 13 December 2015; received in revised form 20 June 2016; accepted 14 August 2016

KEYWORDS
Nanofibers;
Core-shell structures;
Electrospinning method;
Photocatalytic activity;
UV-shielding performance.

Abstract. One-dimensional TiO_2/SiO_2 core-shell nanofibers were fabricated using a single-nozzle co-electrospinning process with phase-separated, mixed polymer composite solution. The core and shell were composed of Polyvinylpyrrolidone (PVP) and Polyacrylonitrile (PAN) polymers with uniform distribution of TiO_2 and SiO_2 nanoparticles (NPs), respectively. The NPs were synthesized via sol-gel reaction, simultaneously, in the respective polymer solutions. The morphologies and structures of the fabricated TiO_2/SiO_2 core-shell nanofibers were investigated by XRD, FTIR, SEM, EDS, and TEM images. The influences of different amounts of TiO_2 and SiO_2 precursors on the photocatalytic and UV-shielding performance of TiO_2/SiO_2 core-shell nanofibers were studied. Photocatalytic activity of the nanofibers was evaluated by observing photo-degradation of Methyl Orange (MO) aqueous solution under irradiation of ultraviolet (UV) light. Our results for the TiO_2/SiO_2 core-shell nanofibers indicate good potential for superior applications in photocatalytic and UV shielding devices.

1. Introduction

Photochemical oxidations for the removal of organic contaminants by Semiconductor Metal Oxides (SMOs) have been widely studied in the literatures [1-6]. Among these, TiO_2 NPs have been more extensively studied for their use in photovoltaic cells, electrochromic materials, photocatalysis, and waste water treatments [5]. Super-fine titanium dioxide particles in the nanometer scale with high transparency have also been used for shielding against a broad range of UV wavelengths [6].

Many studies have confirmed that UV radiation could cause serious damages to eye, skin, immune system, and biological genomes of human being [7,8]. Therefore, the exploration of UV-shielding materials is a hot research topic in materials science and has attracted considerable research interests.

Titanium dioxide is a wide-bandgap (3.2 eV) semiconductor that can absorb UV light and has been widely used in heterogeneous photocatalysis to degrade organic pollutants in water and air [9]. TiO_2 NPs have become a promising photocatalyst due to their chemical stability, low cost, and high photocatalytic activity [9]. However, the major limitations to their commercial applications are the nature of aggregation, difficulty in recycling, and recovery of TiO_2 NPs. To overcome these difficulties, efforts have been made to fabricate one-Dimensional (1D) structures. 1D

*. *Corresponding author. Fax: +98 51 38805000*
E-mail address: nasser@um.ac.ir (N. Shahtahmassebi)

nanocomposites have many excellent characteristics such as faster electron transport, enhanced light absorption and scattering, and larger surface area because of 1D geometry [10].

A number of recent studies have focused on the preparation of polymeric hybrid fibers by incorporating some wide-bandgap semiconductor fillers like TiO_2, ZnS, and ZnO into the polymer matrix. The effect of the incorporated polymers is that, in addition to having a high transparency throughout the visible range, they can strongly absorb the deep-ultraviolet (DUV) wavelengths less than 300 nm [11].

Kwon et al. proved that the UV-blocking efficiency of 1D TiO_2 nanowires and nanotubes was higher than that of commercial TiO_2 NPs, which might be due to their enhanced photo-scattering capability caused by large surface area and their specific band structure [12].

Extensive research has been conducted to develop polymer-matrix composites containing SiO_2 NPs fillers. For instance, formation of SiO_2 NPs incorporated into polyethylacrylic-acid (PEAA) resin by a melt blending process improves the UV-shielding ability. Si-ZnO/PEAA showed about 97% UV-shielding activity, which is more than that of ZnO/PEAA [7]. Also, the studies of Chao-Hua Xue et al. indicated that silica NPs not only improved the UV-shielding property but also upgraded the UV-durability of the super hydrophobicity on the textiles [13]. Moreover, silica (SiO_2) fume enhanced Electromagnetic Interference (EMI) shielding effectiveness of multi-walled carbon nanotube/cement composites [14].

Considering the above studies, SiO_2 NPs in PAN as a shell and TiO_2 in PVP as a core, i.e. TiO_2/SiO_2 core-shell nanofibers, are expected to exhibit enhanced UV-shielding and photocatalytic activities.

PAN is recognized as the most important and promising precursor for carbon fiber. There are numerous advantages for PAN fibers, including high degree of molecular orientation, and higher melting point and thermal stability [15]. It is also possible to blend the PAN with other polymers like PEG (poly ethylene glycol) and PVP [15].

In this work, TiO_2/SiO_2 core-shell nanofibers were synthesized using the co-electrospinning method. Recently, the technique of electrospinning has provided an innovative approach for the straightforward fabrication of 1D nanomaterial with diameter typically ranging from tens to hundreds of nanometers. Electrospinning has become one of the inexpensive, simple, and convenient techniques that use electrostatic force to produce polymeric, ceramics, and composite continuous ultrafine fibers [16].

In the present study, we focused on synthesizing 1D core-shell nanofibers and using PAN and PVP polymers for improving UV-shielding and photocatalytic properties. Such special structures incorporate surface modification of TiO_2 nanofibers by SiO_2 nanofibers and provide a better adsorption, larger specific surface area, and enhancement in the photocatalytic activity.

Meanwhile, TiO_2/SiO_2 nanofibers were fabricated with different amounts of TBOT and TEOS (precursors) for investigating the role of density of NPs in the photocatalytic activity and UV-shielding efficiency. In addition, the UV shielding performance of TiO_2/SiO_2 core-shell nanofibers was compared with those of pure SiO_2 and TiO_2 NPs and our results indicated the superiority of our samples in UV-shielding and photocatalytic applications.

2. Experimental

2.1. Materials

All chemicals were of analytical grade and utilized without further purification. Tetraethylorthosilicate (TEOS), TBOT (Tetra-*n*-butyl-orthotitanate), and acetic acid (glacial) were procured from Merck Co. Polyvinylprrolidone (PVP, Mw = 130000) and Polyacrylonitrile (PAN, Mw=150000) were purchased from Sigma Aldrich Co. and *N*, *N*-dimethylformamide (DMF) was obtained from Scharlau Co. Moreover, TiO_2 NPs from TECNAN Co. were used.

2.2. Synthesis procedure

2.2.1. Preparation of precursors

To prepare the precursor solutions for co-electrospinning, a sol-gel chemical route was applied. First, a solution with different amounts of TEOS and acetic acid was added into 0.7 g of PAN that was dissolved in 5 mL of DMF at room temperature and stirred for 6 h to obtain sheath solution. Meanwhile, different amounts of TBOT and acetic acid were added into 0.7 g of PVP and 5 mL of DMF under vigorous magnetic stirring at 60°C to prepare core solution. Core solution was prepared after being rapidly stirred for 6 h. Finally, equal amounts of two solutions were mixed and magnetically stirred until a homogeneous solution was obtained for the electrospinning process. The amount of chemicals that were used for synthesizing various samples of TiO_2/SiO_2 core-shell nanofibers (**a**, **b**, and **c**) are listed in Table 1.

2.2.2. Single-nozzle co-electrospinning process

The strategy for fabrication of TiO_2/SiO_2 core-shell nanofibers, which basically used single-nozzle co-electrospinning and interface sol-gel reaction, is illustrated in Figure 1(a). Five components (PAN-TEOS and PVP-TBOT-DMF) were required to make the initial core-shell nanofibers separated as continuous and discontinuous phases due to the incompatibility of the two polymers in the mixed solution [17]. The resulting viscous hybrid solution was injected into the electrospinning apparatus by a syringe. In electrospinning process, the high voltage was held at 13 kV, the flow

Table 1. Chemicals used for synthesis of TiO_2/SiO_2 core-shell nanofibers.

Sample	TEOS (mL) (shell solution)	TBOT (mL) (core solution)	Acetic acid (mL) added to core	Acetic acid (mL) added to shell	PVP (g) (core polymer)	PAN (g) (shell polymer)
a	0.7	0.5	1.5	1	0.7	0.7
b	0.8	0.6	1.5	1	0.7	0.7
c	0.9	0.7	1.5	1	0.7	0.7

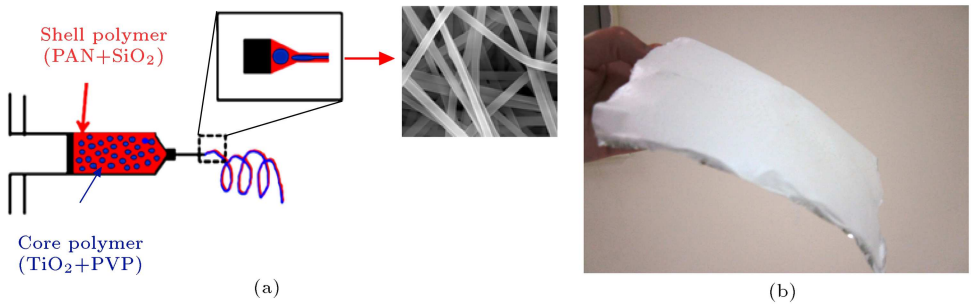

Figure 1. (a) The strategy of fabrication of TiO_2/SiO_2 core-shell nanofibers. (b) Photographic image of the final product that was collected on the aluminum foil.

rate of the syringe pump was 0.4 mL/h, the distance between the nozzle and the collector was 14 cm, and drum linear and rotary speeds were 220 mm/min and 300 rpm, respectively. The fibers were collected on an aluminum foil and dried at 300°C for 1 h. The final product can be seen in Figure 1(b). Core-shell nanofibers were fabricated by using electrospinning device model (eSpinner NF CO-N/VI) from Asian Nanostructures Co, (ANSTCO).

2.3. Photocatalytic activity measurements

To evaluate the photocatalytic performance of TiO_2/SiO_2 nanocomposite nanofibers, Methyl Orange (MO) was used as target organic pollutant for catalytic degradation reaction under UV light irradiation, which was generated by a 125-W mercury lamp. In a typical procedure, for each sample, 10 mL of solution of MB with 20 mg/L of concentration was taken into the vessel and 20 mg of photocatalyst (nanofibers and TiO_2 NPs) was added into the above dye solution. During the photoreaction, the samples were collected at regular intervals (20 min) and centrifuged to remove the photocatalyst. The concentrations of the target organic solution before and after degradation were measured by using a UV-Vis spectrometer (UVD2950). The adsorption capability (q_e) and degradation efficiency (D) of the samples were calculated using the following equations [18,19]:

$$q_e = \frac{(C_0 - C_e)V}{W}, \tag{1}$$

$$D = \frac{C_e - C_t}{C_e} * 100 = \frac{A_e - A_t}{A_e} * 100, \tag{2}$$

where C_0 is the initial concentration of target solution (mg/L); C_e is equilibrium concentration after degradation/adsorption (mg/L); V is the volume of target solution (mL); W is the weight of the synthesized photocatalyst (mg); and, finally, A_0, A_e, and A_t are the corresponding absorbances of dye at the original, equilibrium, and at the time t minutes later, respectively.

2.4. Characterization

The crystallographic structure of the sample was investigated using X-Ray Diffraction (XRD) Advanced Bruker model D8 (using Cu Kα line $\lambda = 0.15406$ nm). X-ray intensity was determined in the ranges of $20° < 2\theta < 80°$ with a 0.5° step size.

Fourier transform infrared (FTIR) spectra were recorded by AVATAR-370-FTIR Thermonicolet FTIR spectrometer.

Transmission Electron Microscopy (TEM) and Scanning Electron Microscopy (SEM) micrographs were used to observe diameters and morphology of the fibers. TEM images of core-shell nanofibers were recorded using a Leo 912AB TEM. The morphologies of the nanocomposite nanofibers were recorded using a Leo 1450VP SEM. For optical studies, the absorption spectra of nanofibers were measured by a UV-Vis spectrophotometer (UVD2950).

3. Results and discussion

3.1. Morphology of electrospun nanofibers

SEM micrographs of TiO_2/SiO_2 core-shell nanofibers (**a**, **b**, and **c** are the samples that were explained in synthesis procedure) are shown in Figure 2.

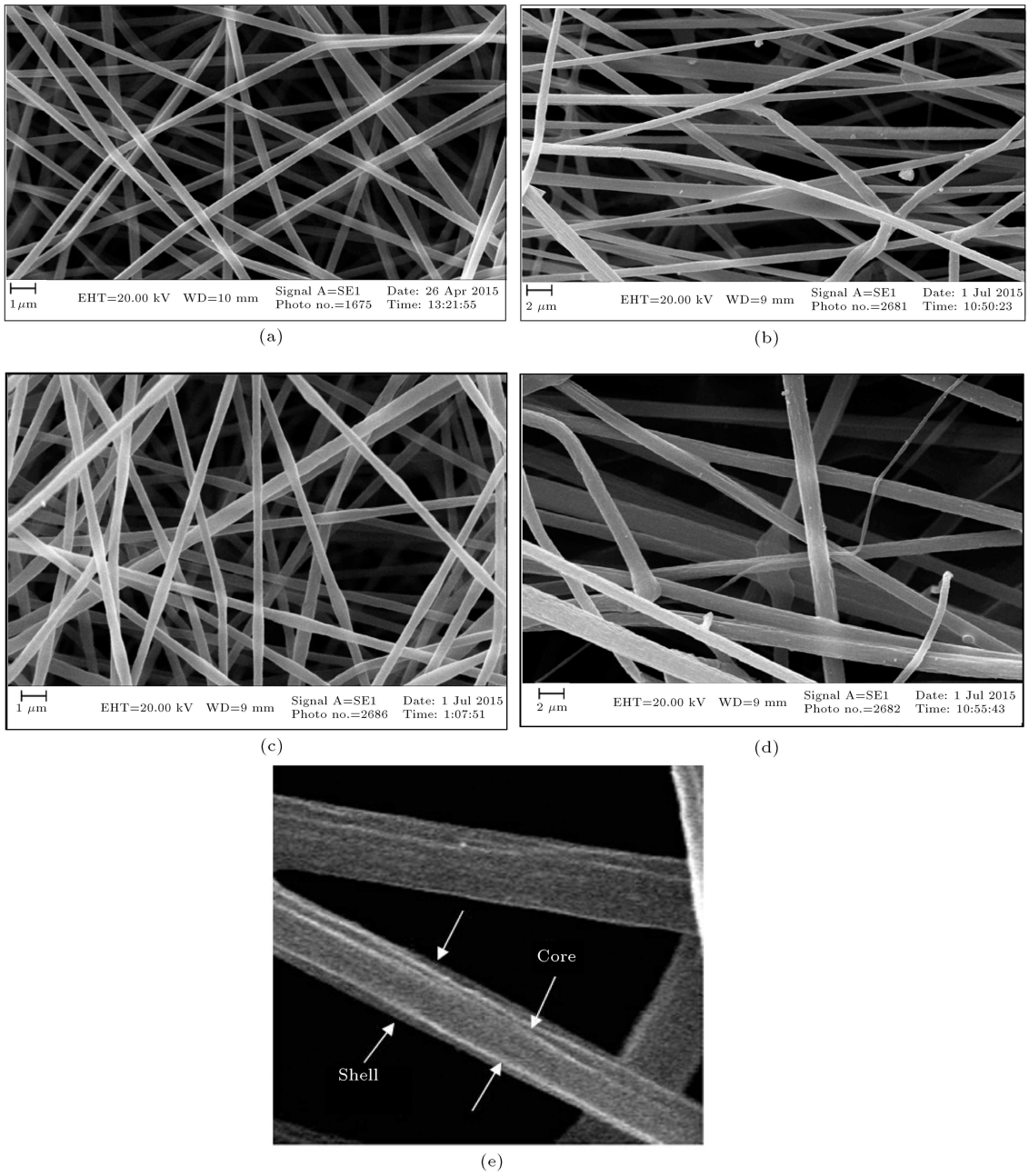

Figure 2. SEM micrographs of TiO_2/SiO_2 core-shell nanofibers: (a) Sample **a**; (b) sample **b**; (c) sample **c**; (d) samples 10000 magnification; and (e) enlarged SEM micrograph of TiO_2/SiO_2 core-shell nanofibers.

As seen in Figure 2, very uniform and smooth fibers without any beads were formed with average diameter ranging from 358-550 nm, which is in very good agreement with reported data in the literature [10,20].

The average diameters of TiO_2/SiO_2 nanofibers were measured by the Image Tool 3.00 software. The average diameters for different samples are summarized in Table 2.

Also, Core-shell structure of nanofibers can be clearly seen in Figure 2(d) and (e). The SEM micrograph with 10000 magnifications was chosen and enlarged. Enlarged SEM micrograph from core-shell structure shows formation of thick core and very fine shell.

Table 2. Full diameter of TiO_2/SiO_2 core-shell nanofibers.

Sample	**a**	**b**	**c**
Diameter (nm)	530	550	358

For further morphological analysis, TEM micrograph was recorded. A TEM micrograph of core-shell nanofibers is displayed in Figure 3 that confirms the successful formation of core-shell structure. TEM

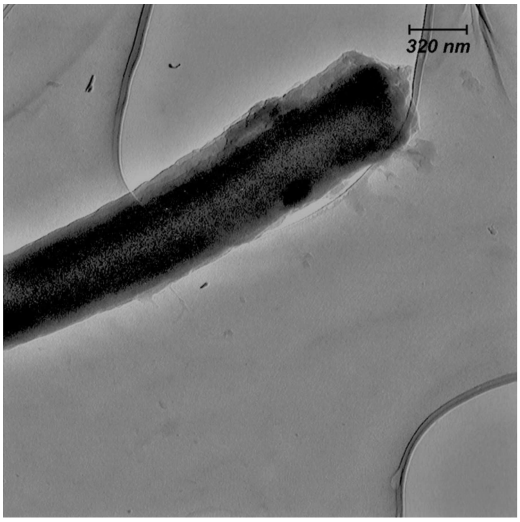

Figure 3. TEM micrograph of TiO_2/SiO_2 core-shell nanofibers.

image shows that very thick core and very fine shell are formed successfully (Figure 3).

The Energy-Dispersive X-ray Spectroscopy (EDS) analysis was employed to determine chemical composition in the samples where the resultant spectra indicated the presence of Si, Ti, O, and C elements in all samples (Figure 4). In all spectra, the presence of Al and Au peaks was attributed to the presence of aluminum foils that were used for collecting fibers, and Au peaks were related to the gold used for coating the sample surface during its preparation steps for SEM characterization. Figure 4(a) shows very weak Si and Ti peaks due to a small amount of precursors (TEOS, TBOT) that was used in synthesis process, and strong C peak is due to PAN and PVP polymers. Figure 4(b) and (c) illustrate stronger Ti and Si peaks that verify existence of more amounts of Si and Ti elements in the fibers.

FTIR spectroscopy studies have been carried out to elucidate the Ti-O and Si-O bonds in the samples (**a**, **b**, and **c**). In all FTIR spectra (Figure 5), strong absorption peak within 550-800 cm^{-1}, which is the typical adsorption in anatase phase of TiO_2, is associated with the stretching vibrations of the Ti-O-Ti bonds [19]. The absorption band at 1095 and 1063 cm^{-1} confirms asymmetric stretching frequency of Si-O-Si linkage and polymeric Si-O vibrations [21]. Figure 6(a) and (b) show chemical structure of PAN and PVP polymers. PAN fibers have many peaks, which are related to the existence of CH_2, C≡N, C=O, C-O, and C-H bonds. Thus, the absorption peaks at 1256, 1388, 1694, 1723, and 2900 cm^{-1} are related to C-O-C, C-C, C-O, C=O, and C-H bonds, respectively [22].

Upon oxidation, the nitrile groups (C≡N) in PAN chain intend to cyclize in the form of –C=N–C=N–. Thus, strong peaks at 1670-1673 cm^{-1} and weak peaks

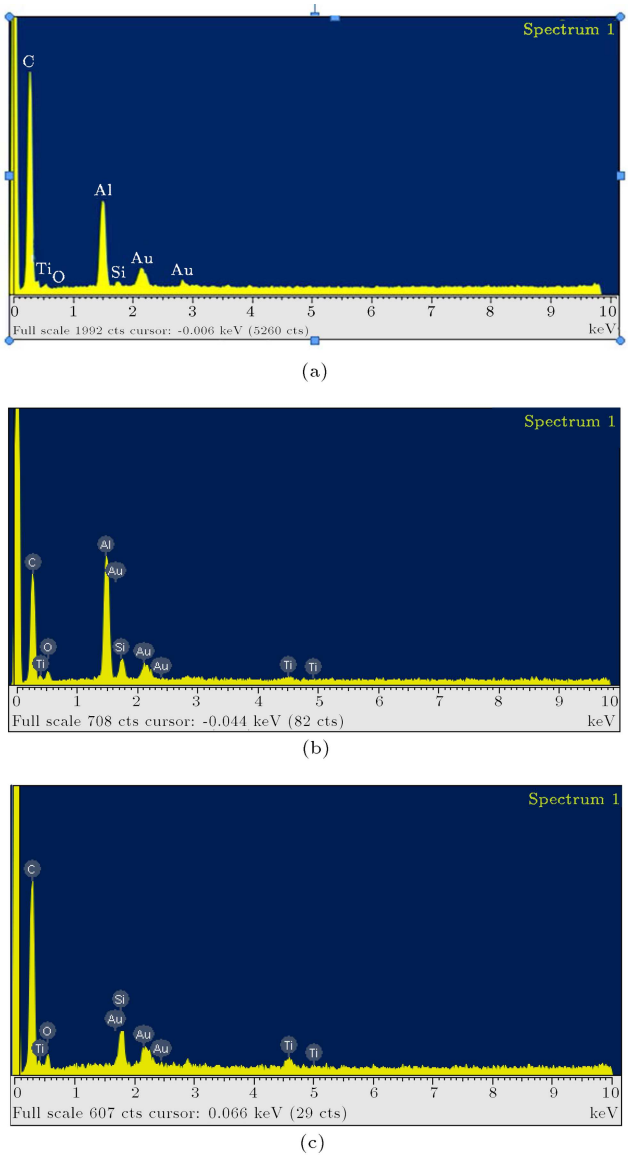

Figure 4. EDS spectra of (a) sample **a**, (b) sample **b**, and (c) sample **c**.

at about 2240 cm^{-1} are related to existence of C-N and C≡N bonds, respectively [23].

The peaks at 3491 cm^{-1} in all the spectra correspond to the stretching vibrations of the –OH group of the absorbed water molecules and the surface hydroxyls on the TiO_2 particles [24]. In addition, FTIR spectrum shows that with increasing the amount of TEOS and TBOT in the synthesis, more intense IR bands are observed.

Crystal structure and phase purity of the synthesized nanofibers were investigated using X-Ray Diffraction (XRD). As seen in Figure 7, XRD pattern of core-shell nanofibers demonstrates that the 1D core/shell nanofibers are made up of anatase TiO_2 core and amorphous SiO_2 shell. The broad peaks indicate that nano-crystalline nature of TiO_2 NPs has formed successfully. The average crystalline size of the NPs

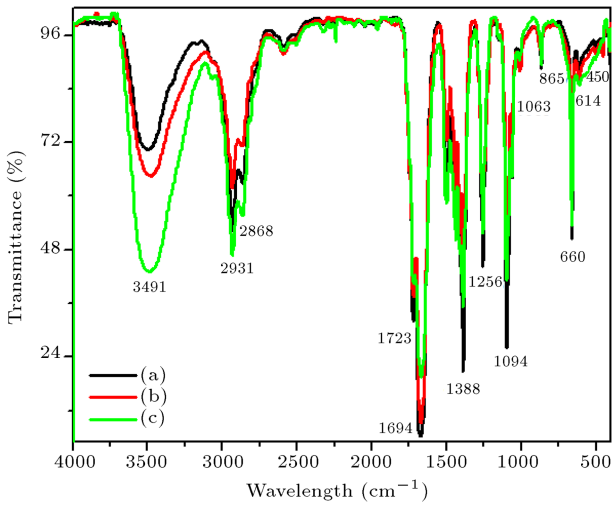

Figure 5. FTIR spectra of (a) sample **a**, (b) sample **b**, and (c) sample **c**.

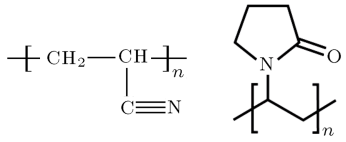

(a) (b)

Figure 6. Chemical structures of (a) PAN polymer and (b) PVP polymer.

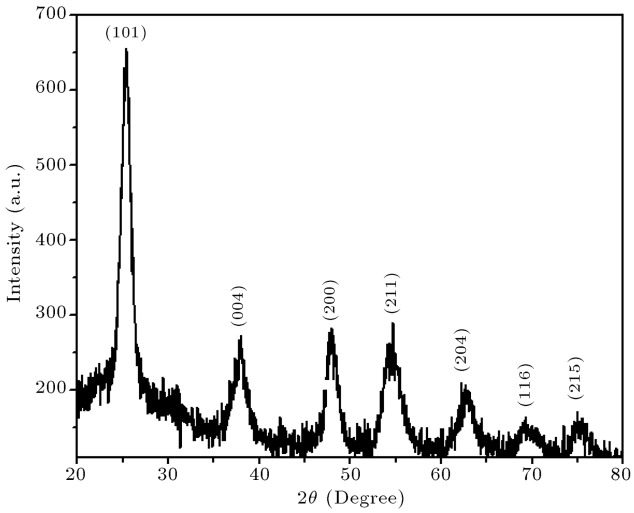

Figure 7. XRD pattern of TiO_2/SiO_2 core-shell nanofibers.

in the polymer matrix was calculated using Scherrer's equation [25,26]. Crystalline sizes were calculated for major peaks, i.e. (204) and (004), whose results are summarized in Table 3.

3.2. UV-shielding and photocatalytic activity of TiO_2/SiO_2 core-shell nanofibers

Recently, many attempts have focused on synthesizing of nanostructures with high UV-shielding efficiency. Different shapes of SiO_2 NPs showed high UV shielding efficiency. For example, mesoporous silica nanospheres reflect more than 90% of the UV and visible light in the wide range of 240-800 nm and more than 70% of the UV light shorter than 240 nm, which are significantly higher than those for the bulk silica [12,27].

Table 3. The obtained structural parameters of XRD analysis for major peaks.

hkl	2θ (deg.)	FWHM (deg.)	DXRD (nm)
204	62.767	2.053	4.8
004	38.007	1.576	5.7

To study UV-shielding ability of core-shell TiO_2/SiO_2 nanofibers, UV-Vis absorption spectra of all the samples (**a**, **b**, and **c**), pure SiO_2, and commercial TiO_2 NPs were measured. (Pure anatase/rutile TiO_2 and SiO_2 NPs with 10 nm of average crystalline size were used for comparison.)

As shown in Figure 8(a), SiO_2/TiO_2 core-shell nanofibers with the highest SiO_2 and TiO_2 precursors (sample **c**) show the best UV-shielding performance, especially in UV and DUV wavelengths. UV-shielding activities of core-shell nanofibers and pure samples in an increasing order are as follows: **a** < SiO_2 NPs < **b** < TiO_2 NPs < **c**.

For better understanding, UV-Vis transmittance spectra of the above samples were also measured (Figure 8(b)). Transmitting efficiency of sample **c** in UV and DUV (ranging from 210 to 250 nm) wavelengths is approximately zero, demonstrating that such nanocomposite nanofibers have excellent UV-prevention performance superior to the commercially TiO_2 NPs and other core-shell nanofibers (samples **b** and **c**). TiO_2/SiO_2 core-shell structure shields all UV and DUV rays completely.

Photo-degradation experiments on MO were carried out for the purpose of studying the degradation capability of the novel photocatalyst on the dyes under UV light irradiation. The degradation mechanism can be interpreted as the following equations:

$$TiO_2 + h\nu \rightarrow TiO_2\left(e_{CB} + h^+_{VB}\right), \quad (3)$$

$$h^+_{VB} + MB \rightarrow \text{Oxidation of MO}, \quad (4)$$

$$h^+_{VB} + H_2O \rightarrow H^+ + \bullet OH, \quad (5)$$

$$h^+_{VB} + OH^- \rightarrow \bullet OH, \quad (6)$$

$$e_{CB} + O \rightarrow \bullet O^-_2, \quad (7)$$

$$\bullet O^-_2 + MO \rightarrow MO - OO\bullet, \quad (8)$$

$$\bullet OH + MO \rightarrow \text{degradation of MO}. \quad (9)$$

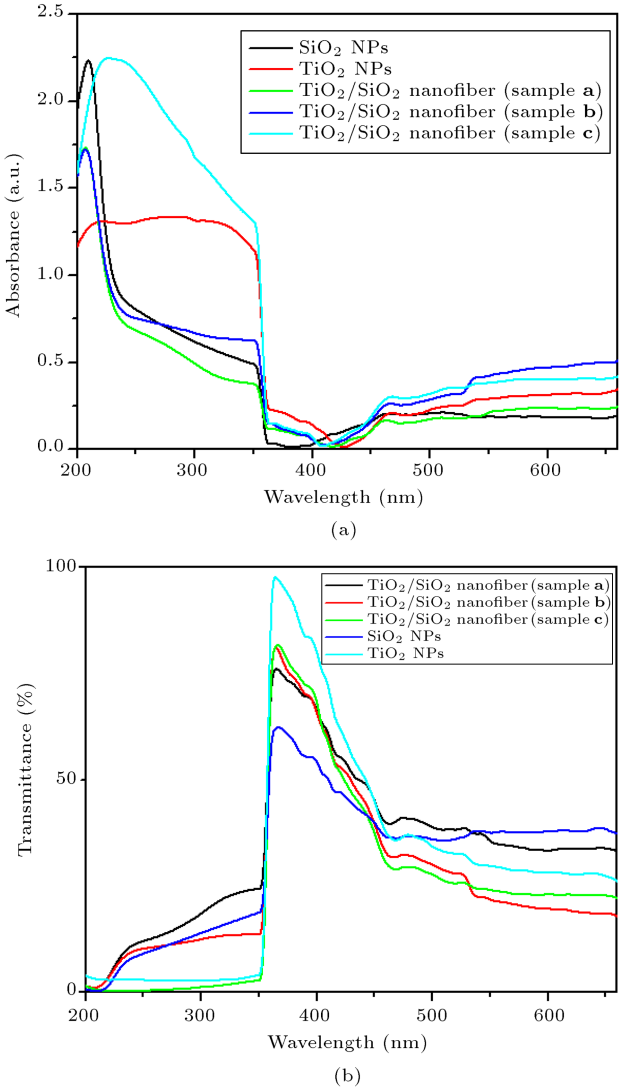

Figure 8. (a) UV-Vis absorbance and (b) UV-Vis transmittance spectra of TiO_2/SiO_2 core-shell nanofibers, pure TiO_2, and SiO_2 NPs.

In Eqs. (3)-(9), h^+_{VB} and e_{CB} occupy an important position in degradation of organic molecules. Photo generation of electron-hole pairs between the conduction (CB) and Valence Bands (VB) due to excitation of TiO_2 under UV light illumination is responsible for the production of hydroxyl radicals and superoxide anion [28]. The process of photocatalytic degradation MO is the same as destroying contamination under UV light in the presence of photocatalyst samples.

Absorption changes spectra of MO aqueous solution in the presence of core-shell nanofibers (samples **a**, **b**, and **c**) under UV-light irradiation can be seen in Figure 9. Spectra were recorded within the time interval of 0-60 min. It was observed that the intensity of the absorption peak of MO decreases as the irradiation time increases. Sample **c** shows the greatest decrease in absorbance of MO solution within 1h and best photo-degradation activity. For further

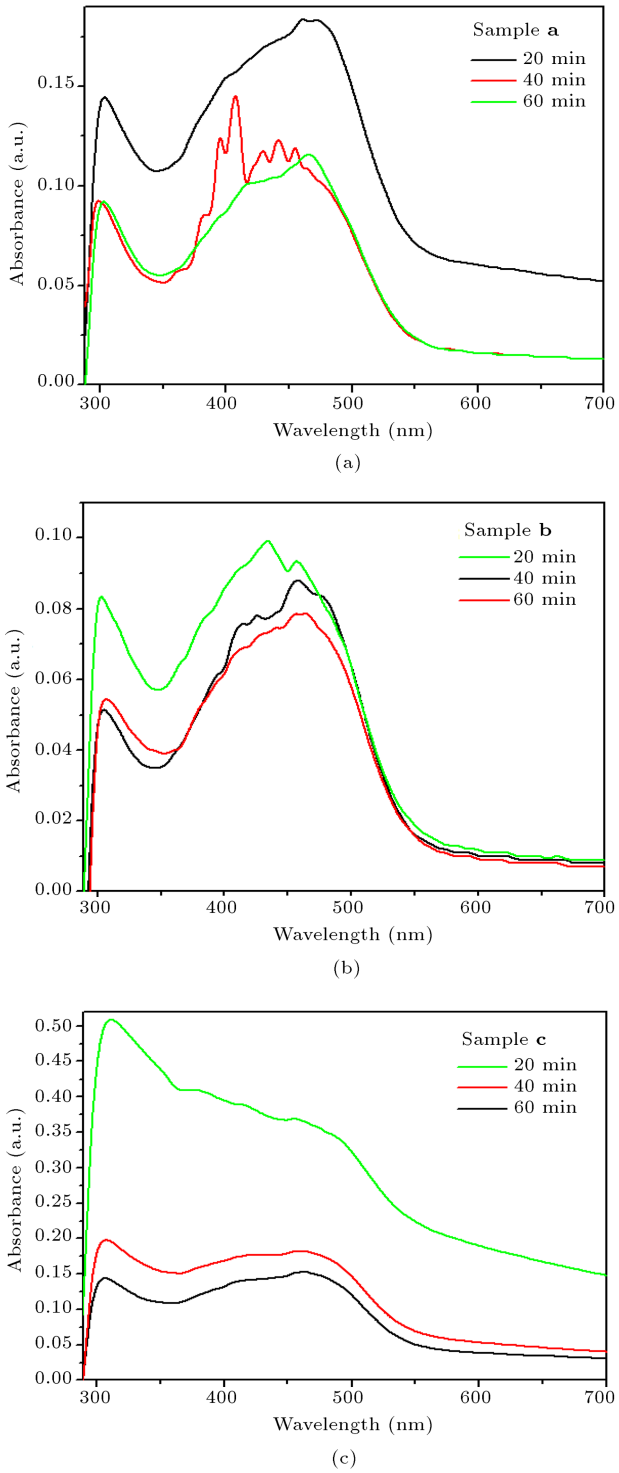

Figure 9. Absorption changes spectra of MO aqueous solution under different UV-irradiation times for (a) sample **a**, (b) sample **b**, and (c) sample **c**.

photocatalyst analysis, degradation rate of MO under UV irradiation was calculated.

Figure 10 demonstrates the rate of MO degradation as a function of time in the presence of photocatalyst, TiO_2/SiO_2 core-shell nanofibers under UV irradiation. The degradation rate (%) was calculated as

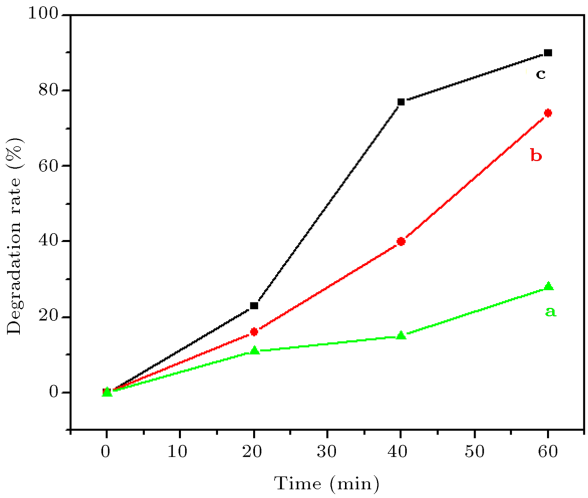

Figure 10. Photocatalytic degradation rate of MO under UV-light irradiation of TiO_2/SiO_2 core-shell nanofibers.

$(C_0 - C/C_0) \times 100$, where C_0 is the initial concentration and C is the concentration at time t [28]. A fast decomposition of MO dye with a rate of 90.3% has been observed within 60 min. The best photocatalytic activity (90.3%) was reached for sample **c** within 60 min. It can be seen that the photocatalytic efficiencies of these samples vary in the following order: sample **a** < sample **b** < sample **c**. The photocatalytic tests for TiO_2 NPs were also carried out for comparison of core-shell nanofibers. Figure 11(a) and (b) show UV-Vis spectrum and degradation rate of MO under UV radiation of TiO_2 NPs, respectively. It can be clearly seen in Figure 11(b) that degradation rate of MO reached about 50% within 60 min that is significantly less than degradation rate of MO in the presence of TiO_2/SiO_2 nanofibers with the highest precursors (sample **c**).

Sample **a** shows very weak photocatalytic activity under UV light radiation; degradation rate of MO for sample **a** reached only 28% within 60 min because of the slight amount of TiO_2 and SiO_2 in TiO_2/SiO_2 core-shell structure.

1D core-shell structure of nanofibers overcomes the aggregation nature, difficulty of recycling, and recovery problem of TiO_2 NPs, and shows excellent photocatalytic activity. Herein, fast photo generation, charge separation, and relatively slow charge recombination occur, which significantly enhance the photocatalytic activity of the as-prepared photocatalyst samples [29].

SiO_2 NPs are one of the strongest known materials in nature that strengthen the stability of the core-shell nanofibers; SiO_2 NPs in the shell part of TiO_2/SiO_2 core-shell structures with increasing surface area of the core fibers can improve photocatalytic activity.

Moreover, PAN and PVP polymers have an important role in photocatalytic performance of core-shell nanofibers. There are some reports showing that PVP and PAN polymers are good templates, which enhance photocatalytic efficiency of tube-brush-like ZnO nanostructures, and BiOBr nanosheets and Fe (III)-amidoximated, respectively [23,30,31].

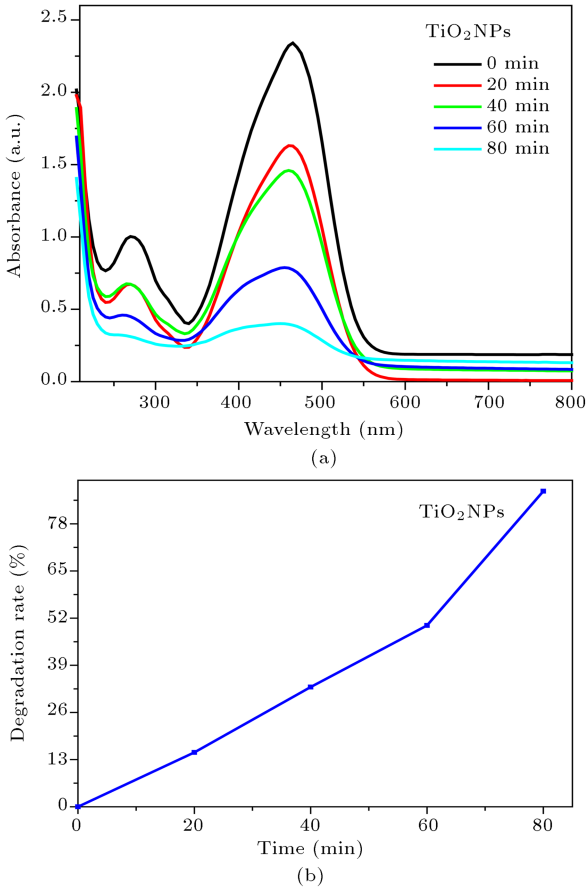

Figure 11. (a) UV-Vis absorbance and (b) photocatalytic degradation rate of MO under UV-light irradiation for of TiO_2 NPs.

PAN and PVP polymer matrixes were used to fabricate a 1D core-shell structure that promoted UV-shielding efficiency and photocatalytic performance of core-shell structure. TiO_2/SiO_2 core-shell nanofibers indicate very good potential for better applications in UV light shielding devices and UV-sensitive materials.

4. Conclusions

In summary, TiO_2/SiO_2 core-shell nanofibers were successfully synthesized using single-nozzle co-electrospinning process and sol-gel approach.

TEM and SEM micrographs illustrate that the intended core-shell structures have formed successfully. Structural properties of as-prepared samples were investigated by XRD, FTIR, and EDS techniques. FTIR spectra illustrate that absorption peaks at 550-800 cm^{-1} and about 1095 cm^{-1} are related to the

existence of Ti-O and Si-O bonds in the samples. Furthermore, EDS characterizations show the presence of C, O, Ti, and Si elements in the core-shell structures.

PAN and PVP polymers were used as a new carrier for TiO_2 and SiO_2 NPs and enhanced UV-shielding activity and photocatalytic performance of TiO_2/SiO_2 core-shell nanofibers. All UV and DUV rays were shielded by TiO_2/SiO_2 core-shell nanofibers with the highest amount of TiO_2 and SiO_2 precursors. UV-Vis transmittances approached almost zero for sample **c**. This unique nanostructure exhibits excellent potential for photocatalytic and UV-shielding application; thus, it can be a good candidate for fabrication coatings with UV-prevention and photocatalytic properties.

References

1. Bayal, N. and Jeevanandam, P. "Synthesis of TiO_2-MgO mixed metal oxide nanoparticles via a sol-gel method and studies on their optical properties", *Ceram. Int.*, **40**(10), pp. 15463-15477 (2014).
2. Zhang, Y., Zhuang, S., Xu, X. and Hu, J. "Transparent and UV-shielding ZnO@PMMA nanocomposite films", *Opt. Mater. (Amst).*, **36**(2), pp. 169-172 (2013).
3. Luo, J., Ma, S.Y., Li, F.M., Li, X.B., Li, W.Q., Cheng, L., Mao, Y.Z. and GZ, D. "The mesoscopic structure of flower-like ZnO nanorods for acetone detection", *Mater. Lett.*, **121**, pp. 137-140 (2014).
4. Saini, P. and Choudhary, V. "Enhanced electromagnetic interference shielding effectiveness of polyaniline functionalized carbon nanotubes filled polystyrene composites", *J. Nanoparticle Res.*, **15**(1), pp. 1415 (2013).
5. Zhang, Y. and Li, P. "Porous Zr-doped SiO_2 shell/TiO_2 core nanoparticles with expanded channels for photocatalysis", *Mater. Des.*, **88**, pp. 1250-1259 (2015).
6. Ukaji, E., Furusawa, T., Sato, M. and Suzuki, N. "The effect of surface modification with silane coupling agent on suppressing the photo-catalytic activity of fine TiO_2 particles as inorganic UV filter", *Appl. Surf. Sci.*, **254**(2), pp. 563-569 (2007).
7. Ramasamy, M., Kim, Y.J., Gao, H., Yi, D.K. and An, J.H. "Synthesis of silica coated zinc oxide-poly(ethylene-co-acrylic acid) matrix and its UV shielding evaluation", *Mater. Res. Bull.*, **51**, pp. 85-91 (2014).
8. Matsumura, Y. and Ananthaswamy, H.N. "Toxic effects of ultraviolet radiation on the skin", *Toxicol. Appl. Pharmacol.*, **195**(3), pp. 298-308 (2004).
9. Guo, N., Liang, Y., Lan, S., Liu, L., Ji, G., Gan, S., Zou, H. and Xu, X. "Uniform TiO_2-SiO_2 hollow nanospheres: Synthesis, characterization and enhanced adsorption-photodegradation of azo dyes and phenol", *Appl. Surf. Sci.*, **305**, pp. 562-574 (2014).
10. Thi, T., Nguyen, T., Hee, O. and Seo, J. "Coaxial electrospun poly (lactic acid)/chitosan (core/shell) composite nanofibers and their antibacterial activity", *Carbohydr. Polym.*, **86**(4), pp. 1799-1806 (2011).
11. Savva, I., Kalogirou, A.S., Chatzinicolaou, A., Papaphilippou, P., Pantelidou, A., Vasile, E., Koutentis, P.A. and Krasia-Christoforou, T. "PVP-crosslinked electrospun membranes with embedded Pd and Cu_2O nanoparticles as effective heterogeneous catalytic supports", *RSC Adv.*, **4**(85), pp. 44911-44921 (2014).
12. Wang, Y., Mo, Z., Zhang, C., Zhang, P., Guo, R., Gou, H., Hu, R. and Wei, X. "Morphology-controllable 3D flower-like TiO_2 for UV shielding application", *J. Ind. Eng. Chem.*, **32**, pp. 172-177 (2015).
13. Xue, C.H., Yin, W., Zhang, P., Zhang, J., Ji, P.T. and Jia, S.T. "UV-durable superhydrophobic textiles with UV-shielding properties by introduction of ZnO/SiO_2 core/shell nanorods on PET fibers and hydrophobization", *Colloids Surfaces A Physicochem. Eng. Asp.*, **427**, pp. 7-12 (2013).
14. Nam, I.W., Kim, H.K. and Lee, H.K. "Influence of silica fume additions on electromagnetic interference shielding effectiveness of multi-walled carbon nanotube/cement composites", *Constr. Build. Mater.*, **30**, pp. 480-487 (2012).
15. Saufi, S., and Ismail, A. "Development and characterization of polyacrylonitrile (PAN) based carbon hollow fiber membrane", *Songklanakarin J. Sci. Technol.*, **24**, pp. 843-854 (2002).
16. Nakhaei, O., Shahtahmassebi, N. and Azhir, E. "Co-precipitation synthesis of CaF_2:Er nanocomposites and photoluminescence characterizations of electrospun polyvinyl alcohol/CaF_2:Er nanofibers", *Indian J. Phys.*, **88**(12), pp. 1245-1250 (2014).
17. Lee, J.S., Kwon, O.S. and Jang, J. "Facile synthesis of SnO_2 nanofibers decorated with N-doped ZnO nanonodules for visible light photocatalysts using single-nozzle co-electrospinning", *J. Mater. Chem.*, **22**(29), p. 14565 (2012).
18. Geng, Q. and Cui, W. "Adsorption and photocatalytic degradation of reactive brilliant red K-2BP by TiO_2/AC in bubbling fluidized bed photocatalytic reactor", *Ind. Eng. Chem. Res.*, **49**(22), pp. 11321-11330 (2010).
19. Ukaji, E., Furusawa, T., Sato, M. and Suzuki, N. "The effect of surface modification with silane coupling agent on suppressing the photo-catalytic activity of fine TiO_2 particles as inorganic UV filter", *Appl. Surf. Sci.*, **254**(2), pp. 563-569 (2007).
20. Kayaci, F., Vempati, S., Ozgit-Akgun, C., Donmez, I., Biyikli, N. and Uyar, T. "Transformation of polymer-ZnO core-shell nanofibers into ZnO hollow nanofibers: Intrinsic defect reorganization in ZnO and its influence on the photocatalysis", *Appl. Catal. B Environ.*, **176**, pp. 646-653 (2015).

21. Qiu, Y., Yin, J., Hou, H., Yu, J. and Zuo, X. "Preparation of nitrogen-doped carbon submicrotubes by coaxial electrospinning and their electrocatalytic activity for oxygen reduction reaction in acid media", *Electrochim. Acta*, **96**, pp. 225-229 (2013).

22. Farsani, R., Raissi, S., Shokuhfar, A. and Sedghi, A. "FT-IR study of stabilized PAN fibers for fabrication of carbon fibers", *World Acad. Sci., Engineering and Technology*, **50**, pp. 430-433 (2009).

23. Liu, C., Li, X., Ma, B., Qin, A. and He, C. "Removal of water contaminants by nanoscale zero-valent iron immobilized in PAN-based oxidized membrane", *Appl. Surf. Sci.*, **321**, pp. 158-165 (2014).

24. Fateh, R., Dillert, R. and Bahnemann, D. "Self-cleaning properties, mechanical stability, and adhesion strength of transparent photocatalytic TiO_2-ZnO coatings on polycarbonate", *ACS Appl. Mater. Interfaces*, **6**(4), pp. 2270-2278 (2014).

25. Nakhaei, O., Shahtahmessebi, N. and Rezaee Roknabadi, M. "Synthesis and characterization of CaF_2 NPs with co-precipitation and hydrothermal method", *J. Nanomed. Nanotechnol.*, **2**(5) (2011).

26. Farimani, M.H.R., Shahtahmasebi, N., Rezaee Roknabadi, M., Ghows, N. and Kazemi, A. "Study of structural and magnetic properties of superparamagnetic Fe_3O_4/SiO_2 core-shell nanocomposites synthesized with hydrophilic citrate-modified Fe_3O_4 seeds via a sol-gel approach", *Phys. E Low-dimensional Syst. Nanostructures*, **53**, pp. 207-216 (2013).

27. Fu, J., Wang, Y. and Zhu, Y. "Broadband and high diffuse reflectivity of hollow mesoporous silica nanospheres and their UV light shielding ability for light-labile peroxides", *Mater. Lett.*, **153**, pp. 89-91 (2015).

28. Khan, R., Shamshi Hassan, M., Uthirakumar, P., Yun, J.H., Khil, M.S. and Lee, I.H. "Facile synthesis of ZnO nanoglobules and its photocatalytic activity in the degradation of methyl orange dye under UV irradiation", *Mater. Lett.*, **152**, pp. 163-165 (2015).

29. Liu, Z., Miao, Y.E., Liu, M., Ding, Q., Tjiu, W.W., Cui, X. and Liu, T. "Flexible polyaniline-coated TiO_2/SiO_2 nanofiber membranes with enhanced visible-light photocatalytic degradation performance", *J. Colloid Interface Sci.*, **424**, pp. 49-55 (2014).

30. Chen, X., Zhai, Y., Li, J., Fang, X., Fang, F., Chu, X., Wei, Z. and Wang, X. "Increased photocatalytic activity of tube-brush-like ZnO nanostructures fabricated by using PVP nanofibers as templates", *Appl. Surf. Sci.*, **319**, pp. 216-220 (2014).

31. Li, Y., Wang, Z., Huang, B., Dai, Y., Zhang, X. and Qin, X. "Synthesis of BiOBr-PVP hybrids with enhanced adsorption-photocatalytic properties", *Appl. Surf. Sci.*, **347**, pp. 258-264 (2015).

Biographies

Omolfajr Nakhaei received her BS and MS degrees from Ferdowsi University of Mashhad, where she is a PhD candidate of Solid State Physics. Her research interests focus on nanoscience, especially in synthesizing nanoparticles, nanocomposites, and nanofibers with unique properties.

Nasser Shahtahmassebi received his BS degree in Physics from Ferdowsi University of Mashhad and PhD degree in Theoretical Condensed Matter Physics from Imperial College London. He is Professor and Head of Nanoresearch Center at Ferdowsi University of Mashhad. His research interests focus on theoretical solid-state physics and nanoscience, especially synthesizing various kinds of nanomaterials with unique properties.

Mahmood Rezaee Roknabadi has PhD degree in Solid-State Physics. He is Professor at Ferdowsi University of Mashhad. His research interests focus on applied physics, theoretical projects in solid-state physics, magnetic material, and nanoscience.

Mohamad Behdani received his PhD degree from Ferdowsi University of Mashhad, where he is a lecturer. His research interests focus on synthesis of magnetic and superconductive materials and nanotechnology.